



## SEISMIC PERFORMANCE OF BUCKLING-RESTRAINED BRACE FOR MIDDLE-RISE TIMBER FRAME STRUCTURE

K. Suzuki<sup>(1)</sup>, S. Nakao<sup>(2)</sup>, R. Sagara<sup>(3)</sup>, Y. Miyata<sup>(4)</sup>

<sup>(1)</sup> Manager, Structure Solutions Department, Constec Engi, Co., Japan, [suzuki-kohei@cons-hd.co.jp](mailto:suzuki-kohei@cons-hd.co.jp)

<sup>(2)</sup> Section Chief, Structure Solutions Department, Constec Engi, Co., Japan, [nakao-sadaharu@cons-hd.co.jp](mailto:nakao-sadaharu@cons-hd.co.jp)

<sup>(3)</sup> Graduate Student, Faculty of Engineering and Design, Hosei University, Japan, [ryota.sagara.9j@stu.hosei.ac.jp](mailto:ryota.sagara.9j@stu.hosei.ac.jp)

<sup>(4)</sup> Assistant Professor, Faculty of Engineering and Design, Hosei University, Japan, [yujiro.miyata.48@hosei.ac.jp](mailto:yujiro.miyata.48@hosei.ac.jp)

### **Abstract**

Various state measures have been taken in Japan to promote the use of timber that has reached the suitable age for logging. Due to effects of these measures, middle-rise large-scale timber buildings that were not so many have been planned. In particular, middle-rise timber frame structures using laminated timber is often planned because it can realize large openings and large spaces. Focusing on the structural characteristics of such timber frame structures, the elastic-plastic restoring force characteristics of the frame are expressed by a bilinear model with slip depending on the characteristics of the column-base and the column-beam joint. The hysteresis loop area of such a bilinear-slip model is smaller than that of a standard bilinear model used in steel structures, and the energy absorption due to the hysteresis of the main frame cannot be expected much. For this reason, if damping can be added to timber frame structures, a reasonable improvement in seismic performance can be realized. On the other hand, timber frame structures are a flexible structure, and it is predicted that large shaking will occur in the building during an earthquake. Therefore, it is extremely important to confirm the seismic response characteristics of timber frame structures.

In this paper, we propose a new device specializing in middle-rise timber frame structures, and show the test results on the seismic performance of the device. The proposed device is a buckling-restrained brace that a low-yield-point steel plate restrained by laminated timbers and a carbon fiber. Specifically, the low-yield-point steel plate is sandwiched between two laminated timbers, and these are integrated by wrapping them with the carbon fiber. In such cases, bolts are often used for integration, but this method tends to occur splitting failure of the laminated timber. In addition, if bolts are used, it is necessary to secure an end distance, which leads to a large dimension. The proposed device is designed to be integrated by wrapping the carbon fiber in order to improve these characteristics. The results of the loading tests show that the proposed device has stable hysteresis characteristics and excellent seismic performance.

*Keywords: Timber Frame Structures; Buckling-Restrained Brace; Carbon Fiber; Hysteresis Curve; Buckling Load*



## 1. Introduction

In recent years, various state measures have been taken in Japan to promote the use of timber that has reached the suitable age for logging. Due to the effects of these measures, medium and large-sized timber buildings have recently attracted attention. In particular, timber frame structures using the glued laminated timber can realize a large opening and a large space, and thus has a possibility of planning a rational architectural plan.

Here, attention is paid to the structural characteristics of the timber frame structures. It is difficult to make the rigid joints such as steel structures and reinforced concrete structures at beam-column joints with timber frame structures, semi-rigid joints that depend on moment resistance joints are generally used <sup>[1]</sup>. Therefore, when a horizontal force is applied to such the timber frame structures, the joints show the properties of a rotational spring, and the inter-story drift angle tends to be larger than that of a rigid frame structure. Further, since the restoring force characteristics of such the rotational springs show slip properties, it is impossible to expect to obtain a stable and large hysteresis energy absorption depending on the elastic-plastic restoring force characteristics of these joints.

Therefore, it is considered that the seismic performance of the timber frame structures can be efficiently improved by reducing the inter-story drift angle and improving the energy absorbing ability. We are working on the development of a new energy absorption system specializing in the timber frame structures for the purpose of realizing these. This system installs a vibration control device in a frame and adds damping to the building depending on the hysteresis performance of the device. Thus, the device used must be adapted to the structural characteristics of the timber frame structures. In this paper, we report the outline of the device and the experimental results.

## 2. Technical summary

### 2.1 Required performance of the device

As described above, in the timber frame structures, the inter-story drift tends to increase. Therefore, the device installed in the frame needs to have a stable restoring force characteristic following large deformation. Also, assuming to carry out a stress analysis of the frame that the device is replaced with an elastic-plastic spring, if the device has a restoring force characteristic close to an ideal elastic-plastic model, the accuracy of the model replacement is good and modeling is simple. Furthermore, since timber structures is lighter in weight than steel structures or reinforced concrete structures, it is desirable that the device is also light in weight.

### 2.2 Summary of the device

The device is a buckling-restrained brace <sup>[2] - [4]</sup> in which a low-yield-point steel plate is used as a core plate and the core plate is restrained in the weak axis using timber material and carbon fiber. Fig. 1 shows a configuration image diagram of the device. The device is made by sandwiching a steel plate processed into a dumbbell shape between a pair of timber materials and winding them with carbon fiber to integrate them. There have been some studies of buckling steel plates with timber materials <sup>[5] - [7]</sup>, but they use bolts to integrate them. In general, timber materials are easily split, and if a bolt hole is drilled, there is a concern that the portion may induce splitting. Further, in order to dispose the bolt, it is necessary to secure an end distance, which leads to an increase in the cross section of the restraining member. The device we propose does not drill a bolt hole for these improvements, but integrates it by winding carbon fiber.

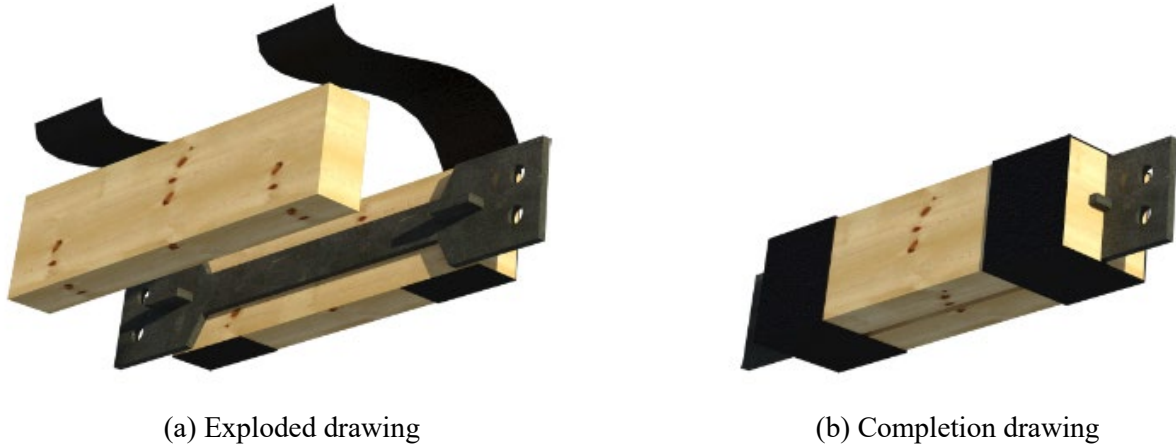


Fig. 1 – Configuration image diagram of the device

### 3. Axial loading tests

#### 3.1 Outline of the tests

##### 3.1.1 Outline of the test specimens

Table 1 shows the parameters of the test specimens. In this tests, a compression test and a tensile test of the core plate, and a gradually increasing cyclic loading test of the device were carried out. The compression test and the tension test were carried out on two each, and the gradually increasing cyclic loading test were carried out on four parameters using the carbon fiber winding method and the clearance between the core plate and the restraining material as parameters. Fig. 2 shows the outline of the test specimens, and Table 2 shows the materials used and its main performance. The core plate used in this test specimen was a steel material processed into a dumbbell shape, and a constricted portion was assumed as a plasticized region. The size of the plasticized region was length  $l$ : 324 mm, width  $b$ : 40 mm, thickness  $t$ : 9 mm, and cross-sectional area  $A_d$ : 360 mm<sup>2</sup>. The grade of the core plate was a low yield point steel LY225, and the yield strength  $\sigma_y$  was 228 N / mm<sup>2</sup> and the tensile strength  $\sigma_u$  was 318 N / mm<sup>2</sup> from the mill test report. Therefore, the yield strength  $N_y$  was 82.1 kN, and the maximum tensile strength  $N_u$  was 114.5 kN. The elastic buckling load  $P_{cr}$  was calculated from the Eq. (1), and was 46.8 kN when the outside of the constriction was assumed to be a rigid region and the constricted end was pin-supported.

$$P_{cr} = \pi^2 E_s I_s / l^2 \quad (1)$$

where,  $E_s$  is Young's modulus of the core plate,  $I_s$  is the sectional moment of inertia about the buckling axis of the core plate.

The buckling restraining member was made of Scotch Pine, identical-grade E95-F315, and was installed so that the lamina was perpendicular to the surface of the core plate. The buckling restraining member was designed to maintain the elastic state even when received to the buckling restraining member design axial force  $dN_{max}$  shown in the Eq. (2), and to satisfy the Eq. (3) so that bending buckling does not occur<sup>[4]</sup>. The buckling load  $N_E^B$  of the buckling restraining member was calculated by equation (4).

$$dN_{max} = d\alpha N_y \quad (2)$$

$$(1 - 1 / n_E^B) m_y^B \geq (a + s + e) / l_B \quad (3)$$

$$n_E^B = N_E^B / dN_{max} \quad (3a)$$

$$m_y^B = M_y^B / dN_{max} l_B \quad (3b)$$

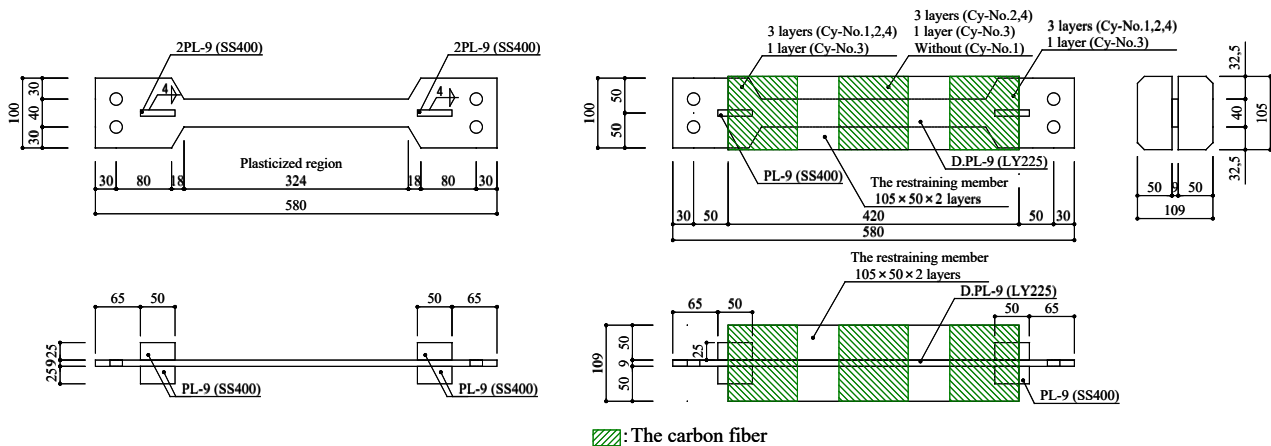


$$N_E^B = \pi^2 E_B I_B / l_B^2 \quad (4)$$

where,  $\alpha$  is the design factor of the buckling restraining member,  $E_B I_B$  is the bending stiffness of the buckling restraining member,  $l_B$  is the length of the buckling restraining member,  $M_y^B$  is the elastic limit moment of the buckling restraining member,  $a$  is the original deflection at the center of buckling restraining member,  $s$  is the clearance between the core plate and the buckling restraining member,  $e$  is the eccentricity of the core plate end.

Table 1 – The parameters of the test specimens

Specimens	Test type	The restraining member	Carbon fiber	Clearance
T – No.1 T – No.2	Tensile test	Without	—	—
Co – No.1 Co – No.2	Compression test	Without	—	—
Cy – No.1 Cy – No.2 Cy – No.3 Cy – No.4	Gradually increasing cyclic loading test	With	3 layers 2 locations 3 layers 3 locations 1 layers 3 locations 3 layers 3 locations	1 mm 0



(a)The core plate

(b)The device

Fig. 2 – Outline of the test specimens

Table 2 – The materials used and its main performance

名称	Grade	Main performance	Remarks
Core plate	LY225	The yield strength $\sigma_y = 228 \text{ N/mm}^2$ The tensile strength $\sigma_u = 318 \text{ N/mm}^2$	From mill test reports
The buckling restraining member	Scotch Pine identical-grade E95-F315	The ending strength $F_b = 31.5 \text{ N/mm}^2$ Young's modulus $E_w = 9,500 \text{ N/mm}^2$ The embedment strength $F_{cv} = 6.0 \text{ N/mm}^2$	Reference strength
Carbon fiber	MRK-M2-30	The fiber weight $300 \text{ g/m}^2$ The tensile strength $\sigma_{fd} = 3,400 \text{ N/mm}^2$ Tensile modulus $E_{fd} = 2.30 \times 10^5 \text{ N/mm}^2$	Reference strength



### 3.1.2 Loading plan

Fig. 3 shows the installation state of the test specimen. The test specimens were installed on one side of the constricted outside part on the actuator and the other side on a fixing jig via a splice plate, and was loaded in the axial direction of the core plate. At this time, a guide rail was provided below the actuator to prevent the actuator from swaying out of the plane of the core plate. As a result, only the axial force acts on the test specimens. The load cycle was controlled by the strain  $\epsilon$  (%) with regards to the plasticized region of the core plate. The strain of 0.05, 0.10, 0.15, 0.20 were loaded for 1 cycle each, and the strain of 0.30, 0.60, 0.75, 1.00, 2.00, 3.00, 4.00, 5.00 were loaded for 2 cycles each.

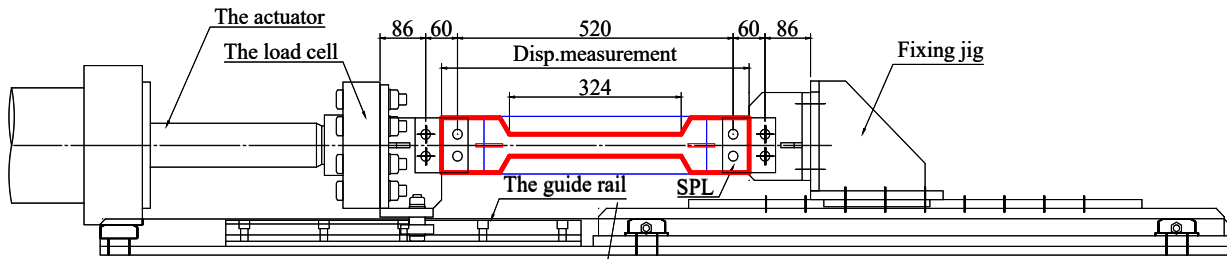
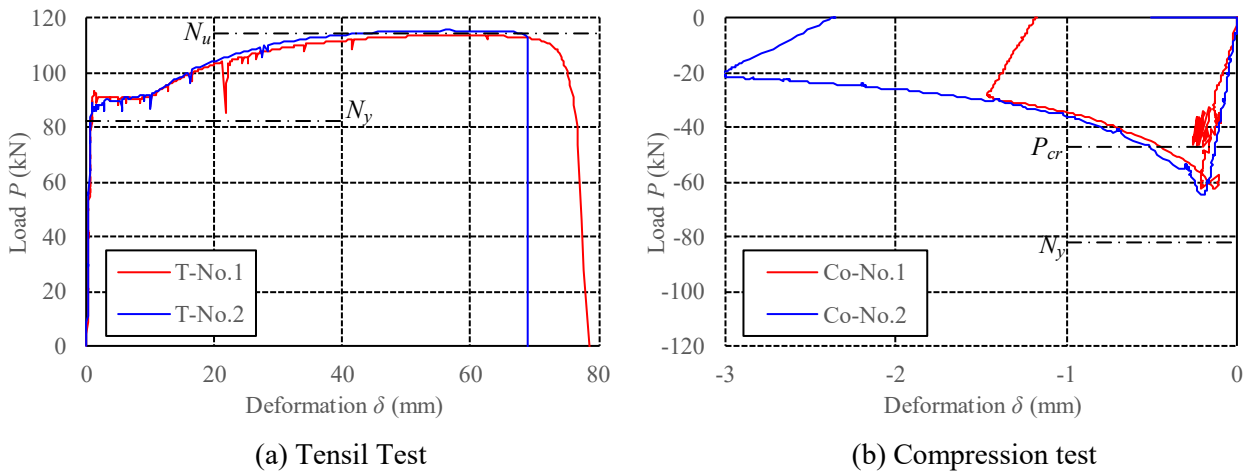


Fig. 3 – The installation state of the test specimen

### 3.2 Test results

#### 3.2.1 The compression test and the tensile test of the core plate

Fig. 4 shows a load-deformation relationship, and Photo 1 shows the failure mode of the test specimens. In the tensile test, the results almost matched the yield strength  $N_y$  and the maximum tensile strength  $N_u$  of the



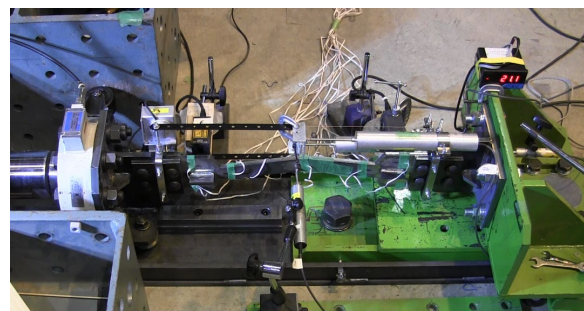
(a) Tensile Test

(b) Compression test

Fig. 4 – Load-Deformation relationship of the core plate



(a) Tensile Test



(b) Compression test

Photo 1 – Failure mode of the core plate



core plate shown in the previous section. In the compression loading test, the compressive strength of both test specimens exceeded the elastic buckling load  $P_{cr}$  according to Eq. (1), with Co-No.1 being 62.5 kN and Co-No.2 being 64.9 kN. When calculating the elastic buckling load  $P_{cr}$ , it was assumed that the constricted end was pin-supported, but it is thought that the fact that it had some rigidity actually was a factor.

### 3.2.2 The gradually increasing cyclic loading test of the device

Fig. 5 shows a load-deformation relationship, and Photo 2 shows failure mode of the test specimens. It was confirmed that all the test specimens exceeded the elastic buckling load  $P_{cr}$  at the time of compressive load and reached the yield strength  $N_y$ . Therefore, the buckling restraining mechanism of this device is considered to be effective. From the load-deformation relationship of Cy-No. 1 to 3, after the compressive load exceeded the yield strength, it decreased slightly and then tended to be retained again. From the failure mode shown in Photo 2, it can be confirmed that all of the core plates of these test specimens buckled and bent out of the plane, resulting cause to embedment behavior into the timber. For this reason, it is considered that the load decreased after the yield strength. In addition, from the load-deformation relationship of Cy-No.1 to 3, although there was no clear difference between the number of winding layers and the number of locations of the carbon fibers, the history of Cy-No.2 was biased to the tensile side. When the failure mode was confirmed, the third-mode-buckling occurred in the core plate of Cy-No.1 and 3, but the local-buckling progressed greatly in Cy-No.2. It is considered that such the difference in the failure mode was reflected in the difference in the hysteresis curve.

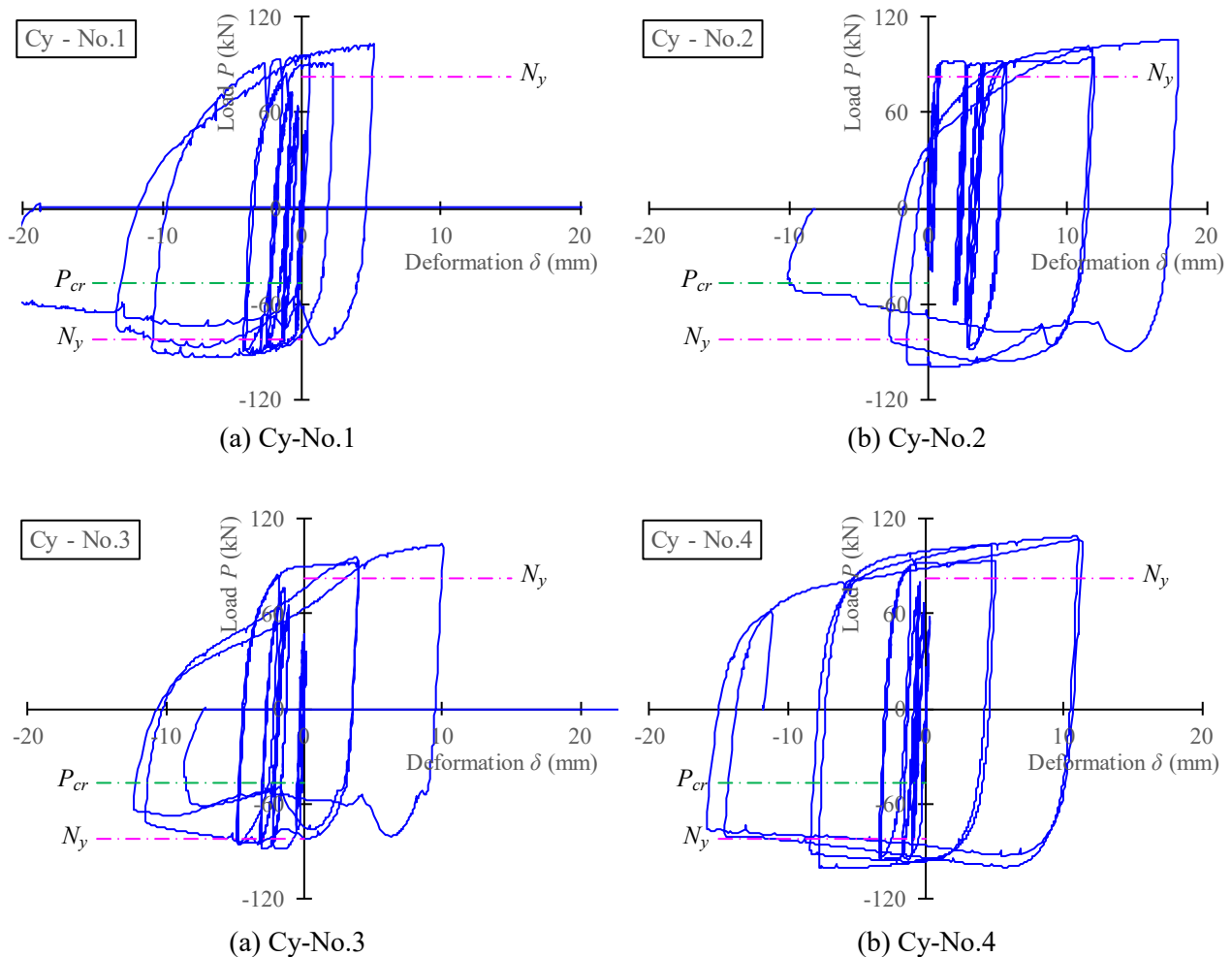


Fig. 5 – Load-Deformation relationship of the device



(a) Cy – No.1



(b) Cy – No.2



(c) Cy – No.3



(d) Cy – No.4

Photo 2 – Failure mode of the device

On the other hand, the load-deformation relationship of Cy-No.4 showed a stable hysteresis curve compared to other test specimens, indicating that it has a high damping performance. From the failure mode, only this specimen did not buckle in the weak axial direction of the core plate, and no embedment into the timber was observed. From this, it was found that the presence of the clearance increased the force by which the core plate pushed the buckling restraining member out of the plane. Furthermore, in the final compressive load, the load gradually decreased after the maximum strength. This is because the first-mode-buckling occurred in the strong axial direction of the core plate. The elastic buckling load in the strong axial direction is 925.1 kN according to Eq. (1), which is much higher than the yield strength. Therefore, buckling in the strong axial direction occurred in the nonlinear region.

#### 4. Conclusions

The outline and basic research results of the new device for improving the seismic performance of a timber frame structures were reported. The knowledge obtained by these are shown as follows.

- (1) The device integrated by sandwiching the steel plate as the core plate with the timber material and winding a carbon fiber thereon exhibits a buckling restraining effect in the weak axial direction of the core plate.
- (2) As a result of the comparison between the presence of the clearance between the core plate and the buckling restraining member, the force of the core plate pushing the buckling restraining member out of the plane increases due to the clearance.
- (3) When a timber material is used as the restraining member, there is a possibility that the core plate may be embedment into the wood.
- (4) When the buckling in the weak axial direction is restrained and the compressive load exceeds the yield strength, nonlinear buckling in the strong axial direction occurs.



## 5. References

- [1] Architectural Institute of Japan (2009): *AIJ Standard for Structural Design of Timber Structures*. 4<sup>th</sup> edition. (in Japanese)
- [2] Takeuchi, T., Wada, A. (2017): *BUCKLING – RESTRAINED BRACES AND APPLICATIONS*, The Japan Society of Seismic Isolation
- [3] Architectural Institute of Japan (2018): *AIJ Recommendations for Stability Design of Steel Structures*. 4<sup>th</sup> edition. (in Japanese)
- [4] Architectural Institute of Japan (2014): *Recommended Provisions for Seismic Damping Systems applied to Steel Structures*. (in Japanese)
- [5] Shibuya, M., Kishiki, S., Yamada, S. (2004): A Study on Stiffening Efficiency of Buckling-Restrained Braces; Part I. Efficiency of wooden Restraint, Architectural Institute of Japan, pp. 873-874 (in Japanese)
- [6] Yoshida, F., Nakagawa, M., Yabuta, T., Nishi, T., Abeyama, T. (2019): Cyclic Loading Test of Buckling Restrained Brace Using Laminated Wood; Part 1 Cyclic Loading Test, Architectural Institute of Japan, pp. 995-996 (in Japanese)
- [7] Haga, Y., Taguchi, T., Shimizu, K., Kondo, T., Kato, M. (2019): Development of the buckling-restrained steel-plate braces using glued laminated timber; Part1: Proposal of Braces and Outline of Basic Tests, Architectural Institute of Japan, pp. 1535-1536 (in Japanese)